Eur. Phys. J. D (2019) 73: 30
https://doi.org/10.1140/epjd/e2018-90566-y

THE EUROPEAN PHYSICAL JOURNAL D

Regular Article

Absolute total cross sections for electron-impact double ionization of He(1s2s ^{3}S) and He$^-$(1s2s2p ^{4}P)*

Matthieu Génévriez[a], Pierre Defrance, Jozo J. Jureta, and Xavier Urbain

Institute of Condensed Matter and Nanosciences, Université catholique de Louvain, Louvain-la-Neuve 1348, Belgium

Received 16 October 2018 / Received in final form 11 December 2018
Published online 7 February 2019

Abstract. We report on the experimental determination of absolute, total cross sections for electron-impact double ionization of helium in its metastable 1s2s ^{3}S state and of the helium negative ion He$^-$(1s2s2p ^{4}P). Cross sections are measured for impact energies ranging from threshold to 1000 eV using the animated crossed beams technique. The fast, pure beam of metastable helium required for the experiment is produced by photodetachment of fast He$^-$ ions. Results for He(1s2s ^{3}S) are compared to those for He(1s^2 ^{1}S), and exhibit similar magnitude and behaviour. The cross section for He$^-$ is large compared to other negative ions and indicates the predominance of indirect ionization channels at large impact energies.

1 Introduction

Double ionization (DI) of atoms and ions by electron impact is subject to a continuous interest since years, essentially from an experimental point of view. Accurate, absolute DI cross sections have been measured for many neutrals, positive and negative ions, including multiply charged ions [1], with impact energies ranging from the reaction threshold up to energies of a few keV. In parallel to these investigations, theoretical approaches were developed in order to identify the various mechanisms at play during direct double ionization (DDI) and elucidate their respective contributions. In a classical picture, there are two so-called two-step (TS) DDI mechanisms. In the first one (TS1), the incident electron ejects a first target electron, which collides with another target electron and ionizes it. In the second one (TS2), the incident electron ejects two target electrons through two successive collisions. In addition, the first electron ejection provokes a sudden change of the atomic potential, which may lead to a second electron ejection during the subsequent relaxation, what is called the shake-off process. The combination of quantum mechanical theoretical calculations accounting for each of the three processes and state-of-the-art experimental investigations able to measure fully differential cross sections provides the most detailed description of DDI [2–5]. For instance, the theoretical works of Dal Capello et al. [4], combined with the experiments of Taouil et al. [3], have established that each of the three identified double ionization mechanisms plays a role in different kinematical conditions for the outgoing electrons (see [6] for a review). Moreover, interference between them must be taken into account in order to interpret the results of the so-called $(e, 3e)$ experiments for double ionization of helium.

Nevertheless, DI is far from been elucidated. Theory has been able to accurately predict the total DDI cross section and the respective importance of the contributing processes only for a limited number of atomic systems [7,8]. In addition to direct processes, indirect double ionization may result from Auger processes, that is, the creation of a hole in an inner shell of the target, which decays by autoionization.

Helium is the simplest atomic system to be subject to DI. The total, absolute DI cross section was measured only for the ground state (1s^2 ^{1}S) [9,10]. Two other states of helium are considered in the present experiment: the 1s2s ^{3}S metastable state of the atom and the 1s2s2p ^{4}P metastable state of the negative ion. The 1s2s ^{3}S state is the lowest excited state of the helium atom, lying 19.82 eV above the ground state [11], and possesses a very long radiative lifetime (7870 s [12]). The 1s2s2p ^{4}P state is the only metastable state of He$^-$, with the lifetimes of its $J = 1/2, 3/2$ and $5/2$ fine structure components being 7.8 μs, 12.3 μs, and 359.0 μs, respectively [13]. All other states are unstable and decay rapidly by autodetachment into a neutral helium atom and a continuum electron. The long lifetime of the 1s2s2p ^{4}P state is explained by the fact that it lies 77 meV below the first excited state of

* Contribution to the Topical Issue "Many Particle Spectroscopy of Atoms, Molecules, Clusters and Surfaces (2018)", edited by Károly Tőkési, Béla Paripás, Gábor Pszota, and Andrey V. Solov'yov.

[a] e-mail: matthieu.genevriez@phys.chem.ethz.ch

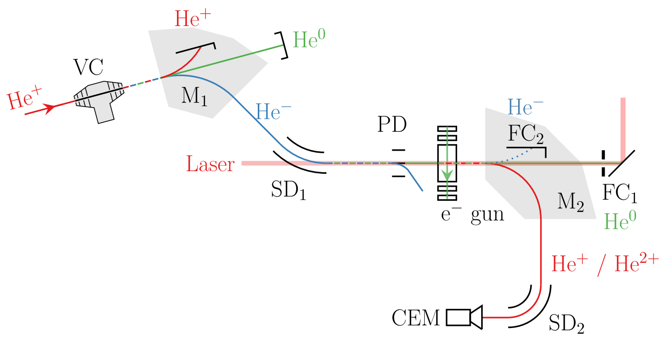

Fig. 1. Experimental setup. VC: sodium vapour cell; M_1: magnetic mass selector; $SD_{1,2}$: spherical deflectors; PD: planar deflector; $FC_{1,2}$: Faraday cup; CEM: channel electron multiplier. For a more detailed sketch of the electron gun setup, see [16].

helium [14], and thus can only decay to the helium ground state. Such a decay is forbidden by spin selection rules, and thus mediated only by weak spin–orbit and spin–spin interactions, resulting in metastability against spontaneous detachment. Theories have demonstrated that DI is very dependent on the correlation between target electrons. For this reason, it is interesting to compare results of DI for situations differing strongly with respect to the ground state. For the ground state, the target electrons are equivalent, while in the present cases non-equivalent target electrons are concerned ($1s2s$ and $2s2p$). In addition, for He^-, an Auger process may result from ejection of the inner-shell electron followed by autoionization of the doubly excited atomic state. For these two systems, absolute double ionization cross sections are measured for impact energies ranging from the reaction threshold to 1 keV. Results are compared with those obtained for the ground state atom.

2 Experimental setup

The experimental setup, shown in Figure 1, is the same as that described in [15]. We therefore give only a brief summary of its main features below.

A fast beam of He^- ions is produced by passing an 8 keV beam of He^+ ions from a duoplasmatron source in a sodium vapour cell, where double charge exchange converts about 1% of the incoming beam into He^-. After the cell, a magnet selects the He^- ions which are then brought to the electron-impact ionization chamber, pumped to high vacuum ($\sim 10^{-10}$ mbar), by a spherical deflector (SD_1). When measuring the electron-impact double ionization cross section of He^-, the planar deflector (PD) shown in Figure 1 is grounded and the laser switched off. The metastability of the $He^-(1s2s2p\ ^4P)$ ion allows one to use conventional beam transport and detection techniques as, for example, the time-of-flight of the ions between the vapour cell and the interaction region ($\sim 3\ \mu s$) is smaller than lifetime of the shortest-lived, $J = 1/2$ fine structure component [13]. In the interaction region, the He^- beam is intersected at right angles by the ribbon-shaped electron beam from a cold-cathode electron gun [16]. After this region, the beam enters a magnetic analyser, which separates its different components. The remaining He^- ions are deflected onto a Faraday cup (FC_2) so that the He^- current can be measured. Currents of 15 nA are routinely achieved. Neutral helium atoms fly straight onto the Faraday cup FC_1. He^+ ions are deflected by the magnetic analyser, reach a spherical deflector (SD_2) and are detected afterwards by a channel electron multiplier (CEM). The experimental setup is carefully designed to ensure complete transmission of the product ions to the CEM [16].

Spurious contributions to the He^+ signal may arise from (i) double ionization of He^- by collision with the residual gas; (ii) ionization of He^- by collision with the residual gas and electron-impact ionization of neutral atoms, and vice-versa; (iii) ionization, either by electron -impact or by collisions with the residual gas, of neutral helium atoms produced by spontaneous detachment of He^-. These contributions are strongly reduced by applying a high-voltage ($\sim$1000 V) bias to the interaction region. In this case, He^+ ions produced when any step of the aforementioned mechanisms occurred outside of the biased region have a different kinetic energy, and are readily filtered out by the magnetic analyser and spherical deflector.

In order to measure the electron-impact double ionization cross section of $He(1s2s\ ^3S)$, one must first tackle issues related to its production. This is a challenging step since standard methods, such as electron-impact excitation or charge-exchange, also leave a significant fraction of atoms in a number of other, undesired states [17]. In a previous study [15], we proposed and implemented a metastable helium source based on the photodetachment of the He^- ion, which produces a beam with excellent purity (>95%). The He^- beam is photodetached by an 8 W, continuous-wave CO_2 laser prior to interaction with the electron beam. The collinear photodetachment geometry (see Fig. 1) allows to reach high neutralisation efficiencies ($\sim$40%) for a modest overlap distance of about 17.5 cm. Just before the interaction region, the remaining He^- ions are deflected out of the beam by a planar deflector (PD), thus leaving a pure beam of metastable helium. The interaction with the electron beam and the analysis of the reaction products proceed as in the case of He^-. The only difference is that the current of metastable atoms cannot be measured directly. Instead, it is determined from the current of secondary electron measured on FC_1, which are emitted upon particle impact on the surface and accelerated outwards by the electric field from a guard electrode. The secondary electron emission coefficient γ, required to obtain the metastable helium current, is calibrated by measuring the attenuation of the He^- current by the laser beam when the planar deflector is switched off [15]. Currents of metastable helium, as measured in amperes, of 6 nA are routinely achieved.

The absolute cross section is measured using the animated crossed beams technique of Defrance et al. [18]. It relies on sweeping, in a linear see-saw motion, the electron beam across the atom or negative ion beam and counting the number of He^{2+} or He^+ ions produced, respectively. The total number K of ions produced during one sweep can then be related to the double ionization cross section

Table 1. Experimental uncertainties arising from systematic effects.

Parameter	Relative uncertainty (%)
CEM detection efficiency η	5
Ion current I_n	1.5
Neutral current I_n	6
Electron current I_e	1.5
Sweeping speed u	1.5
Kinematic factor $\frac{v_e v_n}{\sqrt{v_e^2+v_n^2}}$	0.5

σ as follows,

$$\sigma = \frac{v_e v_n}{\sqrt{v_e^2+v_n^2}} \frac{\mathrm{e}^2}{I_n I_e} \frac{uK}{\eta}, \qquad (1)$$

where v_e and v_n are the velocities of the electrons and atoms or ions, and e is the elementary charge. I_e and I_n are, respectively, the currents of electrons and atoms or ions, u is the sweeping speed of the electron beam and η is the CEM detection efficiency. The strength of the animated crossed beams technique lies in the fact that the form factor, related to the spatial overlap between the electron and atom or ion beams, does not need to be determined. Since, in most cases, the form factor is difficult to measure accurately, this technique allows one to remove an important source of uncertainty in the absolute cross section measurement.

Uncertainties arising from systematic effects are listed in Table 1. When added in quadrature, they give a total, systematic uncertainty of the order of 6% for the double ionization cross section of He^- and 8% for that of He($1s2s$ ^{3}S). The difference between the two uncertainties is due to the additional uncertainty, in the latter case, on the secondary electron emission coefficient γ, required to obtain the neutral current. Statistical uncertainties are, on average, 5% for He^-. Those for He($1s2s$ ^{3}S) reach 20% because of the much smaller cross section and the lower atom beam current. The incident electron energy E_e is corrected for contact potentials and has a spread of about 1 eV. The uncertainty ΔE_e on the absolute energy is estimated to be 0.5 eV.

3 Results

The absolute cross section for electron-impact double ionization of He($1s2s$ ^{3}S) as a function of the electron kinetic energy is listed in Table 2 and presented in Figure 2 along with measured cross sections for double ionization of ground state helium ($1s^2$ ^{1}S) [9,10]. While the onset of the cross section lies lower in energy in the case of metastable helium, because the $1s2s$ ^{3}S state lies 19.82 eV above the ground state, the magnitudes of the cross sections are similar. This violates the classical Thomson scaling law, which states that electron impact ionization cross sections scale as the square inverse of the double ionization potential I_p, and thus predicts a double ionization cross section for the metastable state about 1.8 times larger than that of the ground state. The $1/I_p^2$ scaling is used in most semiempirical formulas describing electron-impact double ionization cross sections [19]. No other experimental or theoretical total cross sections are available for comparison.

Deviation from the Thomson scaling law may be qualitatively understood when taking into account the difference in spin symmetry between the ground- and the triplet metastable states. Electron–electron correlations are expected to be weaker for the triplet metastable state ($1s2s$ ^{3}S) than for the ground or metastable singlet states ($1s^2$ ^{1}S, $1s2s$ ^{1}S) since, as a consequence of the Pauli exclusion principle, the probability for both electrons to be close in space is lowered. In particular, this may lead

Table 2. Absolute cross section for electron-impact double ionization of He($1s2s$ ^{3}S) as a function of electron energy.

E_e (eV)	σ (10^{-19} cm^2)	$\Delta\sigma_{\mathrm{stat}}$ (10^{-19} cm^2)
65	0.06	0.05
70	0.29	0.10
75	0.27	0.08
80	0.47	0.10
90	0.80	0.07
100	1.04	0.16
110	1.24	0.14
120	1.44	0.12
140	1.47	0.17
160	1.46	0.23
200	1.29	0.09
250	1.10	0.10
300	0.94	0.06
350	0.64	0.08
400	0.60	0.05
500	0.52	0.05
600	0.36	0.03
700	0.28	0.07
800	0.22	0.04
1000	0.16	0.04

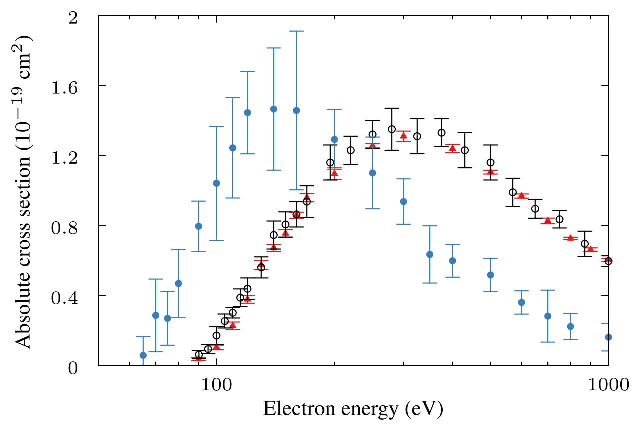

Fig. 2. Absolute cross sections for double ionization of He($1s^2$ ^{1}S) and He($1s2s$ ^{3}S) by electron impact. Full circles: present measurement for He($1s2s$ ^{3}S); full triangles: measurement of Bahati et al. for He($1s^2$ ^{1}S) [10]; empty circles: measurement of Shah et al. for He($1s^2$ ^{1}S) [9]. Error bars give the 2σ statistical uncertainty on the measurements.

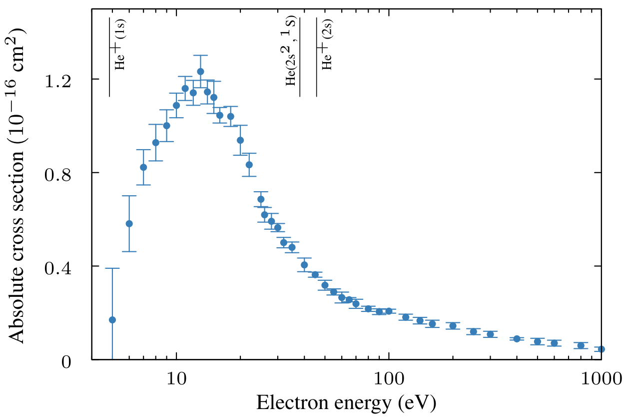

Fig. 3. Absolute cross section for double ionization of He^- by electron impact. The vertical lines indicate the position of various thresholds. Error bars give the 2σ statistical uncertainty on the measurements.

to an important suppression of the TS1 mechanism presented in the introduction, for which the second ionization is the result of a collision between the two electrons of the helium atom. This effect has been predicted theoretically in the case of double photoionization of He($1s^2$ ^{1}S), He($1s2s$ ^{1}S) and He($1s2s$ ^{3}S) [20], where the TS1 mechanism is replaced by its analogue, the knockout mechanism, in which the first ionization is no longer induced by electron impact but by photon impact. Specifically, the relative importance of the knockout and shake-off contributions to the ratio of double- to single ionization cross sections was found to be significantly lower for the triplet state. Following this argument, we may expect the Thomson scaling law to hold for the singlet metastable state, but not for the triplet one. A measurement of the electron-impact double ionization cross section of He($1s2s$ ^{1}S) is therefore desirable.

In the high-impact-energy limit, the double ionization cross section σ behaves as

$$\sigma(E_e) = \frac{1}{E_e}\left(a \ln E_e + b\right), \qquad (2)$$

where E_e is the incident electron kinetic energy [21]. Byron and Joachain also showed that a is a strictly positive quantity related to the integrated double photoionization cross section [21]. Plotting, in a so-called Bethe plot, the product $E_e\sigma(E_e)$ as a function of the logarithm of E_e is therefore a convenient way to investigate the behaviour of the cross section at intermediate and high impact energies. Such plots for the double ionization of ground- and metastable helium are shown in Figure 4a. The coefficient a in equation (2) is expected to be small since the double photoionization cross section of ground state helium is small [22]. The electron-impact double ionization cross section therefore reaches, asymptotically, a plateau. The slight negative slope of the plateau observed in the present results for metastable helium and those of Shah et al. for ground state helium is incompatible with the prediction of Byron and Joachain that $a \geq 0$ [21]. Such a discrepancy was discussed previously [10], however there exists not clear explanation for it.

Table 3. Absolute cross section for electron-impact double ionization of He^- as a function of electron energy.

E_e (eV)	σ (10^{-16} cm^2)	$\Delta\sigma_{\rm stat}$ (10^{-16} cm^2)
5	0.170	0.110
6	0.581	0.060
7	0.822	0.038
8	0.928	0.039
9	1.000	0.034
10	1.087	0.026
11	1.160	0.026
12	1.141	0.027
13	1.232	0.035
14	1.145	0.026
15	1.121	0.034
16	1.045	0.017
18	1.040	0.021
20	0.938	0.032
22	0.833	0.025
25	0.686	0.016
26	0.619	0.016
28	0.591	0.017
30	0.565	0.009
32	0.500	0.011
35	0.480	0.011
40	0.405	0.015
45	0.363	0.005
50	0.318	0.011
55	0.289	0.007
60	0.266	0.012
65	0.256	0.005
70	0.239	0.010
80	0.217	0.006
90	0.205	0.006
100	0.207	0.004
120	0.181	0.006
140	0.167	0.007
160	0.153	0.008
200	0.144	0.007
250	0.120	0.006
300	0.108	0.007
400	0.089	0.003
500	0.077	0.007
600	0.070	0.006
800	0.060	0.006
1000	0.044	0.005

The absolute cross section for electron-impact double ionization of He^- is listed in Table 3 and shown in Figure 3. The double ionization threshold lies low in energy ($\sim$4.84 eV) because of the low binding energies of both He^- (77 meV) and He($1s2s$ ^{3}S) (4.77 eV) [11,14]. The cross section is about three orders of magnitude larger than that for double ionization of helium (see Fig. 2), and is also larger than those of other, light, atomic negative ions [23]. This is not particularly surprising since He^- is a fragile system with a hollow-core electronic configuration. No other experimental or theoretical data are available for

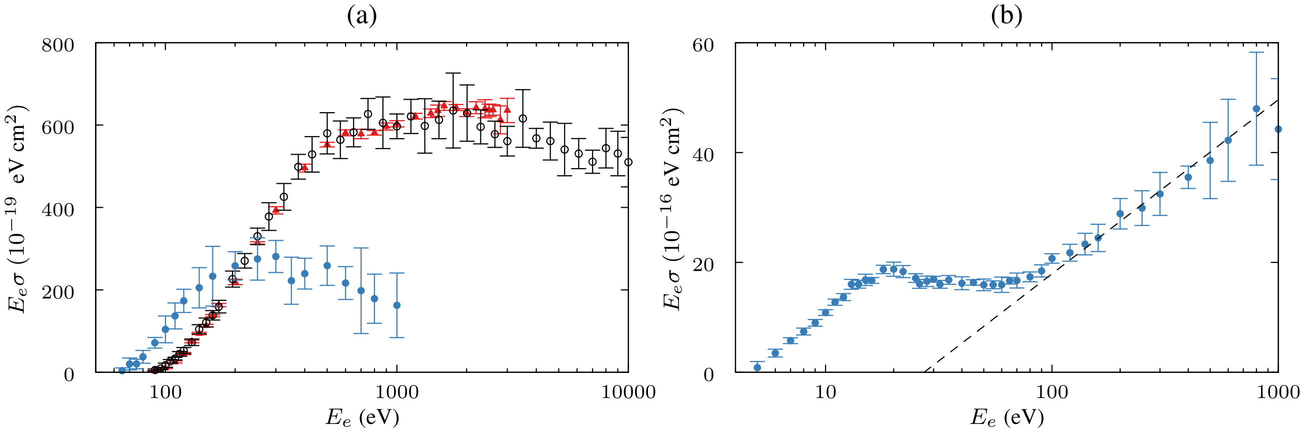

Fig. 4. Bethe plots of the absolute electron-impact double ionization cross sections of: (a) He($1s2s$ ^{3}S) and He(1s^2); (b) He$^-$. Symbols attribution in panel (a) is as in Figure 2. The dashed line in (b) indicates the slope expected for electron-impact single ionization of ground state He$^+$ (see text). Error bars give the 2σ statistical uncertainty on the measurements.

comparison. Semiempirical formulas, such as those proposed by Bélenger et al. [23] or Rost and Pattard [24], do not reproduce satisfactorily the present results, possibly indicating the importance of indirect double ionization channels.

The presence of strong, indirect ionization channels is also suggested by the shape of the Bethe plot of the double ionization cross section presented in Figure 4b. As for ground- and metastable helium, it is characterized by a sharp rise just above threshold followed by a plateau region. However, at higher impact energies (≥70 eV), a second rise is observed which persists up to the highest energy we measured (1000 eV). Such a rise may be attributed to an ionization–autoionization mechanism. Indeed it suffices, in an independent electron picture, to ionize the 1s electron of the He$^-$($1s2s2p$ ^{4}P) ion to be left with a neutral helium atom in a doubly excited state, which further autoionizes, thus producing an He$^+$ ion. This process corresponds to a *single* electron-impact ionization event, whose cross section is expected to be much larger than that of direct double ionization for sufficiently large impact energies. The slope of the second rise in Figure 4b must thus be close to the one expected for electron-impact single ionization of He$^+$($1s$), keeping in mind that small deviations may arise due to the presence of the outer $2s$ and $2p$ electrons in the case of He$^-$. The dashed line in Figure 4b represents the cross section calculated with equation (2) taking $a = 13.77 \times 10^{-16}$ eV cm^2 and $b = -45.5 \times 10^{-16}$ eV cm^2. The value of a was calculated using the expression given by Rudge [25],

$$a = \frac{I_H}{\pi\alpha}\int_0^{\infty}\frac{\sigma_p(E_p)}{I+E_p}\mathrm{d}E_p, \tag{3}$$

where I_H is the ionization potential of hydrogen, α is the fine structure constant, I is the ionization potential of He$^+$($1s$) and E_p stands for the photon energy. The photoionization cross section σ_p of He$^+$($1s$) was calculated from the analytical formula for the dipole matrix elements given by Bethe and Salpeter [26]. The value for b was arbitrarily chosen so that the curve overlaps the experimental results, allowing for easier comparison. One readily observes that the slope associated with the experimental results matches that predicted by theory for single ionization of He$^+$($1s$), thus confirming the attribution of the second rise to the ionization–autoionization mechanism.

4 Conclusion

The absolute cross sections for electron-impact double ionization of the helium atom in its metastable $1s2s$ ^{3}S state and of the helium negative ion were measured for impact energies ranging from threshold to 1000 eV using the animated crossed beams technique. The He$^-$ beam was produced by double charge capture of fast He$^+$ ions in sodium vapour and the pure, fast beam of metastable helium by subsequent photodetachment of the He$^-$ beam. The cross section for double ionization of He$^-$($1s2s2p$ ^{4}P) is large compared to other negative ions, a consequence of its very small binding energy and its hollow-core electronic configuration. Two different ionization regimes are clearly observed in the Bethe plot of the cross section. At low energies, direct double ionization of the two outer electrons dominates, while at higher energies ionization of the 1s core electron followed by autoionization becomes more important. The cross section for double ionization of He($1s2s$ ^{3}S) is similar in magnitude to that of ground state helium ($1s^2$ ^{1}S), a fact that violates the classical Thomson scaling law, and exhibits a similar behaviour in the high impact energy region. The present study thus extends knowledge on the double electron-impact ionization of helium by considering a different, excited initial state and the case of the helium negative ion. Further experimental and theoretical investigations would be most interesting to extend the detailed picture now available for the ground state to the present cases. Finally, we may stress that it is well-known that electron-impact double ionization cross sections depend critically on electronic correlations in the target atom or ion [21]. This is even more crucial in the case of He^-, because even its mere metastability is the result of subtle correlation effects, and the double ionization of He^- may therefore represent an interesting challenge for theory.

The authors thank the Belgian State for the grant allocated by Royal Decree for research in the domain of controlled thermonuclear fusion. This work was supported by the Fonds de la Recherche Scientifique–FNRS through IISN grant No. 4.4504.10.

Author contribution statement

All the authors were involved in the preparation of the manuscript. All the authors have read and approved the final manuscript.

References

1. M. Hahn, A. Müller, D.W. Savin, Astrophys. J. **850**, 122 (2017)
2. A. Dorn, R. Moshammer, C.D. Schröter, T.J.M. Zouros, W. Schmitt, H. Kollmus, R. Mann, J. Ullrich, Phys. Rev. Lett. **82**, 2496 (1999)
3. I. Taouil, A. Lahmam-Bennani, A. Duguet, L. Avaldi, Phys. Rev. Lett. **81**, 4600 (1998)
4. C. Dal Cappello, R. El Mkhanter, P. Hervieux, Phys. Rev. A **57**, R693 (1998)
5. A. Dorn, A. Kheifets, C.D. Schröter, B. Najjari, C. Höhr, R. Moshammer, J. Ullrich, Phys. Rev. Lett. **86**, 3755 (2001)
6. J. Berakdar, A. Lahmam-Bennani, C. Dal Cappello, Phys. Rep. **374**, 91 (2003)
7. M.S. Pindzola, F. Robicheaux, J. Colgan, J. Phys. B: At. Mol. Opt. Phys. **39**, L127 (2006)
8. P. Liu, J. Zeng, J. Yuan, J. Phys. B: At. Mol. Opt. Phys. **51**, 075202 (2018)
9. M.B. Shah, D.S. Elliott, P. McCallion, H.B. Gilbody, J. Phys. B: At. Mol. Opt. Phys. **21**, 2751 (1988)
10. E. Bahati, H. Cherkani-Hassani, P. Defrance, J.J. Jureta, T. Kereselidze, Z. Machavariani, I. Noselidze, J. Phys. B: At. Mol. Opt. Phys. **38**, 1261 (2005)
11. A. Kramida, Y. Ralchenko, J. Reader, NIST ASD Team, NIST Atomic Spectra Database (2016), http://www.nist.gov/pml/data/asd.cfm
12. S.S. Hodgman, R.G. Dall, L.J. Byron, K.G.H. Baldwin, S.J. Buckman, A.G. Truscott, Phys. Rev. Lett. **103**, 053002 (2009)
13. P. Reinhed, A. Orbán, J. Werner, S. Rosén, R.D. Thomas, I. Kashperka, H.A.B. Johansson, D. Misra, L. Brännholm, M. Björkhage et al., Phys. Rev. Lett. **103**, 213002 (2009)
14. P. Kristensen, U.V. Pedersen, V.V. Petrunin, T. Andersen, K.T. Chung, Phys. Rev. A **55**, 978 (1997)
15. M. Génévriez, J.J. Jureta, P. Defrance, X. Urbain, Phys. Rev. A **96**, 010701 (2017)
16. J. Lecointre, D.S. Belic, H. Cherkani-Hassani, J.J. Jureta, P. Defrance, J. Phys. B: At. Mol. Opt. Phys. **39**, 3275 (2006)
17. T.J. Gay, in *Atomic, Molecular, and Optical Physics: Atoms and Molecules*, edited by F. Dunning, R.G. Hulet (Academic Press, 1996), Vol. 29, Part B, Chap. 6, pp. 95–114
18. P. Defrance, F. Brouillard, W. Claeys, G. van Wassenhove, J. Phys. B: At. Mol. Phys. **14**, 103 (1981)
19. M. Zambra, D. Belic, P. Defrance, D.J. Yu, J. Phys. B: At. Mol. Opt. Phys. **27**, 2383 (1994)
20. A. Emmanouilidou, T. Schneider, J.M. Rost, J. Phys. B: At. Mol. Opt. Phys. **36**, 2717 (2003)
21. F.W. Byron, C.J. Joachain, Phys. Rev. **164**, 1 (1967)
22. J.A.R. Samson, W.C. Stolte, Z.X. He, J.N. Cutler, Y. Lu, R.J. Bartlett, Phys. Rev. A **57**, 1906 (1998)
23. C. Bélenger, P. Defrance, E. Salzborn, V.P. Shevelko, H. Tawara, D.B. Uskov, J. Phys. B: At. Mol. Opt. Phys. **30**, 2667 (1997)
24. J.M. Rost, T. Pattard, J. Phys. B: At. Mol. Opt. Phys. **32**, L457 (1999)
25. M.R.H. Rudge, Rev. Mod. Phys. **40**, 564 (1968)
26. H.A. Bethe, E.E. Salpeter, *Quantum Mechanics of One- and Two-Electron Atoms* (Springer, Boston, MA, 1977)